(helical surface currents oriented downwind) (*16*), the downwelling currents at the convergence zone over internal waves may pull less buoyant fractions of an oil spill under water, making the spill inaccessible for cleanup operations. Finally, oil caught in the convergence zone could kill or injure (*17*) the larvae that are often concentrated there (*4, 5*).

REFERENCES AND NOTES

1. T. Maxworthy, *J. Geophys. Res.* **84**, 338 (1979).
2. M. Rattray, Jr., *Tellus* **12**, 54 (1960).
3. T. K. Chereskin, *J. Geophys. Res.* **88**, 2649 (1983).
4. A. L. Shanks, *Mar. Ecol. Prog. Ser.* **13**, 311 (1983).
5. M. J. Kingsford and J. H. Choat, *Mar. Biol.* **91**, 161 (1986).
6. S. Turner, *Buoyancy Effects in Fluids* (Cambridge Univ. Press, Cambridge, 1973).
7. D. M. Brown and L. Cheng, *Mar. Ecol. Prog. Ser.* **5**, 225 (1981).
8. The set of internal waves was manifested at the surface as alternating bands of glassy and rippled water, the bands were oriented parallel to shore, and the entire set was moving onshore. The surface waters over the convergence zone are characterized by strips of glassy water and enhanced surface roughness, with the rough region leading the glassy water in phase. At low wind speeds, the rough water is not apparent and convergence zones are delineated simply by strips of glassy water. The characteristics of the convergence zone are due to the combined effects of wave-current interaction over the internal wave [B. A. Hughes and H. L. Grant, *J. Geophys. Res.* **83**, 443 (1978)] and the dampening of surface waves by natural oils concentrated in the convergence [G. Ewing, *J. Mar. Res.* **9**, 161 (1950)]. This set of features is characteristic and unique to tidally generated internal waves (as described by Ewing in the above reference). The surface signature of internal waves has been observed in satellite images of the South Atlantic Bight (*10, 15*), and I have often observed the surface manifestations of internal waves in the water near the Beaufort Inlet.
9. R. S. Arthur, *Deep-Sea Res.* **2**, 129 (1954).
10. C. Sawyer, *NOAA Tech. Memo. ERL PMEL-46* (1983), pp. 1–70.
11. The "catching" efficiency of internal waves was assumed to be equal to the percentage decrease in abundance of tar balls behind the set of internal waves relative to their abundance in front of the set, that is, [1 − (number of tar balls behind the waves divided by number in front)] × 100.
12. R. A. Smith, J. R. Slack, T. Wyant, K. J. Lanfear, *U.S. Geol. Surv. Open-File Rep. 80-687* (1980).
13. S. K. Liu and J. J. Leendertse, *Proceedings of the International Symposium on the Mechanics of Oil Slicks* (International Association for Hydraulic Research, the Netherlands, 1981), pp. 249–265.
14. J. R. Apel, H. M. Byrne, J. R. Proni, R. L. Charnell, *J. Geophys. Res.* **80**, 865 (1975).
15. L.-L. Fu and B. Holt, *Jet Propul. Lab. Publ. 81–120* (1982), pp. 1–200.
16. S. Leibovich and J. L. Lumley, "A theoretical appraisal of the joint effects of turbulence and of Langmuir circulations on the dispersion of oil spilled on the sea" (Report no. CG-D-26-82, Office of Research and Development, U.S. Coast Guard, Department of Transportation, Washington, DC, September 1981).
17. E. D. S. Corner, *Adv. Mar. Biol.* **15**, 289 (1978).

28 August 1986; accepted 23 December 1986

Aromatic Cross-Links in Insect Cuticle: Detection by Solid-State ^{13}C and ^{15}N NMR

JACOB SCHAEFER,* KARL J. KRAMER, JOEL R. GARBOW, GARY S. JACOB,† EDWARD O. STEJSKAL,‡ THEODORE L. HOPKINS, ROY D. SPEIRS

Cross-polarization magic-angle-spinning nuclear magnetic resonance spectroscopy has been used to determine insect cuticle composition and cross-link structure during sclerotization or tanning. Unsclerotized cuticle from newly ecdysed pupae of the tobacco hornworm, *Manduca sexta* L., had a high protein content with lesser amounts of lipid and chitin. Concentrations of chitin, protein, and catechol increased substantially as dehydration and sclerotization progressed. Analysis of intact cuticle specifically labeled with carbon-13 and nitrogen-15 revealed direct covalent linkages between ring nitrogens of protein histidyl residues and ring carbons derived from the catecholamine dopamine. This carbon-nitrogen adduct was present in chitin isolated from cuticle by alkaline extraction and is probably bound covalently to chitin. These data support the hypothesis that the stiffening of insect cuticle during sclerotization results primarily from the deposition of protein and chitin polymers and their cross-linking by quinonoid derivatives of catecholamines.

THE INSECT EXOSKELETON IS A COMplex extracellular cuticular structure whose chemical nature and physical properties vary with functional demands. It is composed primarily of protein, chitin, and water, the interactions of which, although poorly understood, largely determine structural and mechanical properties (*1*). During sclerotization (strengthening), the cuticle becomes stiffer, drier, and resistant to chemical and physical degradation. It has been proposed that catecholamines act as dehydrating agents, protein denaturants, and precursors of cross-linking agents for the presclerotized protein-chitin matrix (*2*). Proposed cross-linking intermediates include *o*-quinones or *p*-quinone methides, whose formation from catechols is catalyzed by oxidative enzymes in the newly secreted cuticle.

Because tanned cuticle is an intractable material and the putative cross-linking agent or agents are highly reactive and transient, the analytical techniques used in the past to study the chemistry of sclerotization have not yielded convincing proof for the cross-linked structures or proposed intermediates. However, recent studies of bacterial cell walls (*3*) have shown that the relatively new solid-state spectroscopic method, cross-polarization magic-angle-spinning (CPMAS) nuclear magnetic resonance (NMR) (*4*), makes it possible to evaluate cross-linked structures in intact biological tissue.

We report here the results of experiments in which CPMAS ^{13}C and ^{15}N NMR were used to determine in situ the relative concentrations of and covalent interactions among catecholamine, protein, and chitin in pupal cuticle of the tobacco hornworm, *Manduca sexta* L. The analytical method depends on the ability to identify and quantitate in intact cuticle the natural-abundance ^{13}C levels, as well as ^{13}C–^{15}N covalent bonds, between catechols or chitin labeled with ^{13}C and protein enriched in ^{15}N-histidine.

At ecdysis, *M. sexta* pupal cuticle is soft and colorless except for small tanned areas on the abdomen (*5*). In a few hours the cuticle stiffens and becomes dark brown. The natural-abundance ^{13}C CPMAS NMR spectra of cuticle can be used to estimate concentration changes of the major organic components during cuticular tanning or sclerotization (*6*). Protein carbons contribute to ^{13}C resonances (lines) 1, 2, 4, 5, and 10 to 16 (*7*) (Fig. 1C and Table 1). The broad peptide backbone α-carbon peaks between 55 and 62 parts per million (ppm) (lines 10 and 11) generally diagnose protein levels (*8*). The well-resolved sharp lines between 74 and 104 ppm (lines 6 to 9) are due to the 2-acetamido-2-deoxy-D-glucopyranoside (GlcNAc) carbons and so reflect chitin content. The oxygenated aromatic carbon

J. Schaefer, J. R. Garbow, G. S. Jacob, E. O. Stejskal, Physical Sciences Center, Monsanto Company, 800 North Lindbergh Boulevard, St. Louis, MO 63167.
K. J. Kramer, U.S. Grain Marketing Research Laboratory, Agricultural Research Service, U.S. Department of Agriculture, 1515 College Avenue, Manhattan, KS 66502, and Department of Biochemistry, Kansas State University, Manhattan, KS 66506.
T. L. Hopkins, Department of Entomology, Kansas State University, Manhattan, KS 66506.
R. D. Speirs, U.S. Grain Marketing Research Laboratory, Agricultural Research Service, U.S. Department of Agriculture, Manhattan, KS 66502.

*Present address: Department of Chemistry, Washington University, St. Louis, MO 63130.
†Present address: Department of Biochemistry, University of Oxford, Oxford OX1 3QU, England.
‡Present address: Department of Chemistry, North Carolina State University, Raleigh, NC 27695.

peak at 144 ppm (line 3) monitors catechols, and the sharp methylene carbon peak at 30 ppm (line 14) can be used to estimate amounts of lipid. Fast cross-polarization rates for protonated carbons, long proton rotating-frame lifetimes, and high concentrations of protons ensure representative relative NMR intensities under the conditions used in these experiments (*8*). When required, absolute concentrations of carbons can be determined by comparison with an external standard.

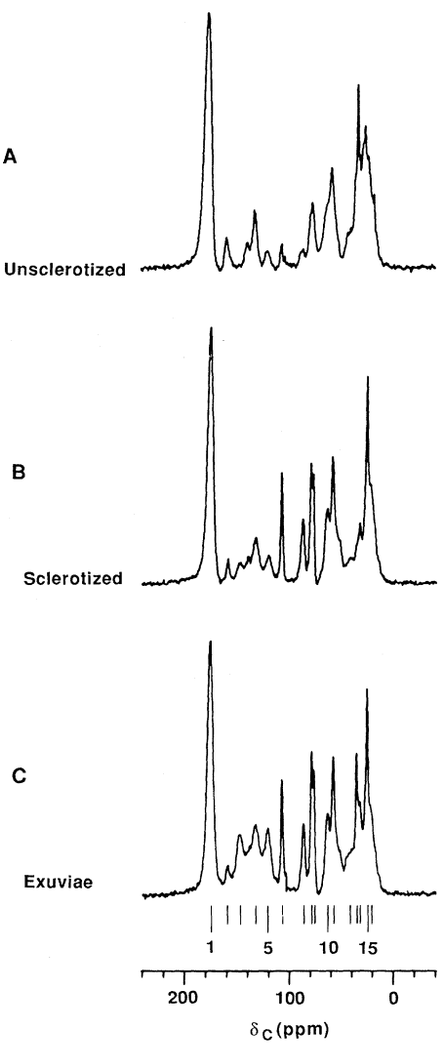

Fig. 1. Natural-abundance CPMAS ^{13}C NMR spectra of (**A**) newly ecdysed and relatively unsclerotized *M. sexta* pupal cuticle, (**B**) 3-day-old sclerotized pupal cuticle, and (**C**) pupal exuviae consisting primarily of highly sclerotized exocuticle. Assignments for lines 1 to 16 are given in Table 1. The scale is in parts per million downfield from tetramethylsilane (TMS) as an external reference. Spectra were obtained at 50.3 MHz through the use of 2-msec cross-polarization transfers from protons and 50-kHz radio-frequency fields. The dried samples were contained in a cylindrical double-bearing rotor spinning at 3.2 kHz. Residual spinning sidebands were suppressed by pulse techniques. Additional details and references may be found in (*8*).

As the cuticle sclerotizes, proteins become progressively less soluble (*9*); the relative levels of protein, chitin, and catechol increase; and those of lipid and water decrease (*10*) (Fig. 1, A and B). The outer heavily sclerotized portion of the cuticle or exuvium contains approximately twice as much protein, 18 times as much chitin and catechol (Fig. 1C), and one-ninth as much water as unsclerotized cuticle does (*10*).

Since the proteins in sclerotized cuticle are difficult to extract, it has long been believed that they are stabilized by cross-links involving covalent bonds to other cuticular components (*1, 2*). Nitrogen-containing amino acid side chains in cuticular proteins are potential nucleophiles for the formation of carbon-nitrogen cross-links with components such as quinonoid intermediates. Our CPMAS ^{15}N NMR spectral data (*7*) of *M. sexta* pupal cuticle labeled by injection of L-[1,3-$^{15}N_2$]histidine into wandering-stage larvae (*11*) support the formation of carbon-nitrogen cross-links. The ^{15}N NMR spectrum of unsclerotized cuticle shows protonated and nonprotonated histidyl ring nitrogen peaks at 140 and 225 ppm, respectively (Fig. 2A), as well as a natural-abundance amide nitrogen peak at 100 ppm. In 3-day-old sclerotized cuticle, a new histidyl signal is observed at 155 ppm that builds up during the time course of sclerotization (Fig. 2B) and becomes the major nitrogen resonance in pupal exuviae (Fig. 2C). The dipolar dephasing produced by delayed ^1H decoupling (*12*) has little effect on the new signal (Fig. 2D), which shows the nitrogen to be nonprotonated. Its chemical shift indicates a histidyl nitrogen attached to either an aliphatic or aromatic carbon (*13*). From the relative intensity of the new peak, it is estimated that one-third to one-half of all histidyl residues in exuviae have undergone a posttranslational substitution to a structure (I) of the form

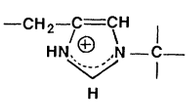

I

Preliminary ^{15}N NMR results involving labeling by [ε-^{15}N]lysine suggest that the ε-amino nitrogen of lysine also forms carbon-nitrogen cross-links in *M. sexta* pupal cuticle, although these are less numerous than the histidyl nitrogen cross-links.

Proteins with substituted histidyl nitrogens seem to be tightly coupled to chitin in sclerotized cuticle. The ^{15}N NMR spectrum of pupal chitin prepared by alkali extraction (*14*) from exuviae labeled with [1,3-$^{15}N_2$] histidine shows only two peaks: a natural-abundance amide peak at 100 ppm and the substituted histidyl ring nitrogen peak at about 150 ppm (Fig. 3A). Delayed decoupling experiments (*12*) on this material demonstrate that the 150-ppm peak consists of two equal components, one protonated and shifted 1 to 2 ppm upfield, and the other nonprotonated and shifted slightly downfield. This result is consistent with the shifts expected (*15*) for the substituted ring structure shown above. About one-third of the total ^{15}N label in the intact cuticle (determined by integration of the spectrum) was recovered in the chitin preparation, which means that virtually all of the substituted histidyl rings are coupled to chitin. These rings remain bound to chitin but are no longer part of the cuticular proteins that have been hydrolyzed away (*14*).

The natural-abundance ^{13}C NMR spectrum of the pupal chitin preparation confirms the presence of aromatic or olefinic carbons (Fig. 3C). However, the total inten-

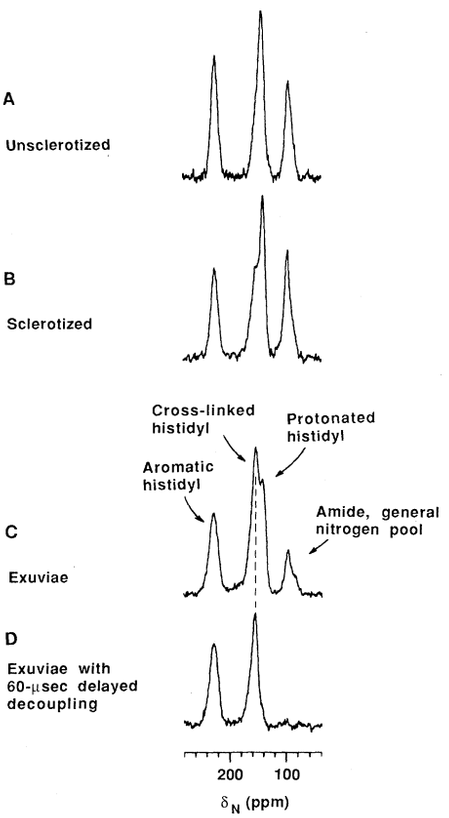

Fig. 2. CPMAS ^{15}N NMR spectra of L-[1,3-$^{15}N_2$]histidine–labeled (**A**) newly ecdysed unsclerotized pupal cuticle, (**B**) 3-day-old sclerotized pupal cuticle, (**C**) pupal exuviae, and (**D**) pupal exuviae under delayed decoupling. Spectra were obtained at 20.3 MHz through the use of matched spin-lock cross-polarization transfers with 1-msec contacts and 35-kHz radio-frequency fields. Only nonprotonated nitrogen resonances survive delayed decoupling. The vertical display for the top two spectra is approximately twice that of the bottom two. The horizontal scale is in parts per million downfield from solid ammonium sulfate as an external reference.

sity of the aromatic carbon peaks between 120 and 160 ppm is 3% of the integrated intensity of the ^{13}C NMR spectrum and so cannot be accounted for exclusively by the ring carbons of histidyl residues (*16*). Therefore, aromatic compounds like catechols must also be present in the chitin preparation. Prolonged exposure of this preparation to hot basic solution eventually leaves only chitin (Fig. 3, B and D).

The proteins coupled to pupal chitin do not seem to be bonded directly. This conclusion is based on the results of double cross-polarization (DCP) MAS ^{13}C NMR experiments, which were used to detect the presence of ^{13}C–^{15}N bonds (*17*). A DCP experiment separates by difference (*18*) those ^{13}C atoms adjacent to ^{15}N atoms from all other ^{13}C atoms. For example, with L-[1,3-$^{15}N_2$]histidine, only the three carbons in the imidazole ring bonded to ^{15}N atoms are detected by DCP signals (Fig. 4A), whereas all carbons in histidine are detected by single cross-polarization signals (Fig. 4B). The intensities of these three carbon DCP peaks can be used to identify the individual ^{13}C–^{15}N bonds in the labeled histidine (*17*). The DCP ^{13}C NMR spectrum of sclerotized cuticle from adults reared from larvae fed uniformly labeled [^{13}C]glucose (*19*) and injected with L-[1,3-$^{15}N_2$]histidine has difference signals at 180 and 140 ppm (Fig. 4C). The intensity of the 180-ppm DCP difference signal relative to that of the normal signal (Fig. 4D) (a ratio of 0.001) arises from the natural-abundance ^{15}N (0.3%) of the amide nitrogens (*20*) in chitin (labeled to 8% ^{13}C by the glucose) and proteins. We attribute the weak DCP difference signals at 140 ppm to natural-abundance ^{13}C adjacent to labeled [^{15}N]histidyl nitrogens (*21*). The absence of any other DCP difference signal rules out direct histidyl nitrogen linkages to chitin carbon atoms.

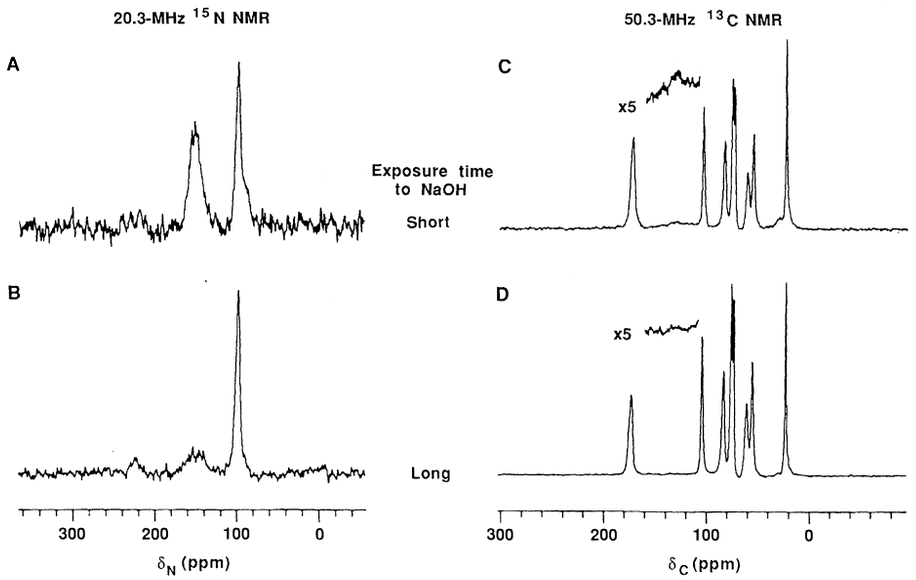

Fig. 3. CPMAS ^{15}N NMR (**A** and **B**) and ^{13}C NMR (**C** and **D**) spectra of chitin extracted by alkali treatment from L-[1,3-$^{15}N_2$]histidine–labeled sclerotized *M. sexta* pupal cuticle. The natural-abundance ^{15}N 100-ppm amide peak (A and B) and the eight major natural-abundance ^{13}C peaks (C and D) all arise from chitin.

The C–N cross-links in *M. sexta* cuticle are formed instead between histidyl ring nitrogens and catecholic ring carbons. The DCP difference ^{13}C NMR spectrum of pupal exuviae from larvae injected with both L-[1,3-$^{15}N_2$]histidine and [*ring*-$^{13}C_6$]dopamine (*22*) shows a peak at 135 ppm, slightly upfield from the major oxygenated ring carbon peak at 144 ppm (Fig. 4, E and F). This peak does not appear in DCP spectra of exuviae labeled only with L-[1,3-$^{15}N_2$]histidine. The 135-ppm chemical shift is consistent with an aromatic carbon next to nitrogen (*23*). Although the exact structure of the histidyl-catecholamine ring adduct is unknown, the data of Figs. 2, 3, and 4 are consistent with a product (see structure **II**, where R = CH_2–CH_2–NH_3^+) from an *o*-quinone sclerotization mechanism (*1, 2*). By this mechanism a cross-link results from nucleophilic attack of the 1- or 3-nitrogen of the imidazole ring on the 2-, 5-, or 6-ring carbon of an *o*-quinone derivative of *N*-β-alanyldopamine. *N*-β-Alanyldopamine is the major catecholamine derived from dopamine found in tanning *M. sexta* pupal cuticle (*24*). A catecholamine-chitin carbon-oxygen

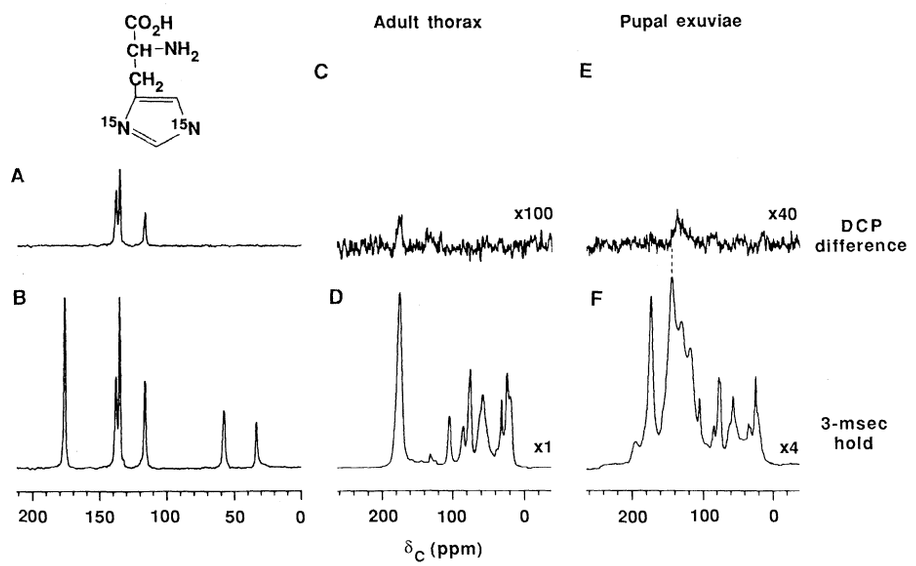

Fig. 4. Single (bottom) and double (top) CPMAS ^{13}C NMR spectra of L-[1,3-$^{15}N_2$]histidine (**A** and **B**), thoracic cuticle of *M. sexta* adults labeled with L-[1,3-$^{15}N_2$]histidine and [^{13}C(U)] glucose (**C** and **D**), and *M. sexta* pupal exuviae labeled with [1,3-$^{15}N_2$]histidine and [*ring*-$^{13}C_6$]dopamine (**E** and **F**). Only ^{13}C atoms directly coupled to ^{15}N atoms have resonances in the double-CPMAS (DCP) difference spectra. The ^{13}C label from glucose appears predominantly in chitin (D), while that from dopamine enhances the intensity of the aromatic region of the spectrum between 120 and 160 ppm (F). Data accumulation involved 35,000 scans (A and B), 400,000 scans (C and D), and 900,000 scans (E and F), respectively. The last of the three accumulations was a 2-week experiment. The histidine sample weighed 470 mg; the thorax sample, 346 mg; and the exuviae sample, 161 mg.

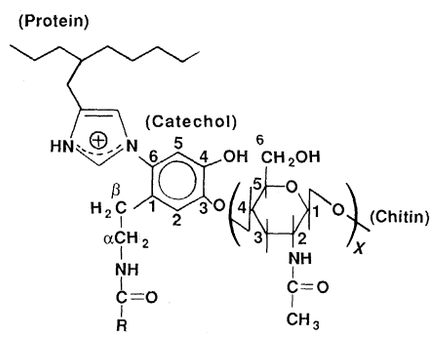

Table 1. Chemical assignments of resonances (*7*) in the CPMAS ^{13}C NMR spectra of *M. sexta* cuticle.

Resonance	δ-Value (ppm)*	Assignment
1	172	Carbonyl carbon in chitin, protein, lipid, and catechol
2	155	Phenoxy carbon in tyrosine; guanidino carbon in arginine
3	144	Phenoxy carbons in catechols
4	131	Aromatic carbons
5	121	Tyrosine carbons 3 and 5; imidazole carbon 4; catechol carbons 2 and 5
6	104	GlcNAc carbon 1
7	85	GlcNAc carbon 4
8	75	GlcNAc carbon 5
9	74	GlcNAc carbon 3
10	62	GlcNAc carbon 6; amino acid α-carbon
11	55	GlcNAc carbon 2; amino acid α-carbon
12	44	Amino acid and catechol aliphatic carbons
13	33	Amino acid, catechol, and lipid aliphatic carbons
14	30	Lipid aliphatic carbons
15	23	Methyl carbons in chitin, protein, lipid, and catechol amino acid methyne carbons
16	19	Amino acid and lipid methyl carbons

*δ-Values relative to external TMS reference.

linkage is drawn between the phenoxy carbon 3 and the GlcNAc carbon 4, but phenoxy carbon 4 as well as other GlcNAc carbons may participate in the conjugate linkage. If we assume that cuticular proteins have a random distribution of residues, of which about 10% are histidines, then the most heavily cross-linked exuviae examined have a histidine-catechol-chitin coupling once every 20 units along the protein chain—a high cross-link density (*25*). Except for the covalent bonding of catechols with sulfhydryl groups in proteins, the formation of catechol adducts with either protein nucleophilic side chains or chitin residues has been little studied (*26*).

Additional direct cross-links between histidyl ring nitrogens and the β-carbon of dopamine may form as a result of a β-sclerotization mechanism where an acyl dopamine with an α, β-unsaturated side chain or a *p*-quinone methide structure is the reactive intermediate (*2*). However, the DCP ^{13}C NMR spectrum of pupal exuviae from fifth-instar larvae injected with both L-[1,3-$^{15}N_2$]histidine and β-[^{13}C]dopamine was too weak to permit an unambiguous assignment of any DCP difference peak, even after a 10-day data accumulation. Most of the ^{13}C label from dopamine appeared in a carbon with a chemical shift of 78 ppm, which indicates the formation of an oxygenated β-^{13}C adduct (*23*) such as *N*-β-alanylnorepinephrine, which is found at levels of micromoles per gram in pupal exuviae (*24*), or perhaps a β-carbon-O-alkylated adduct between *N*-β-alanyldopamine and a seryl, threonyl, tyrosyl, aspartyl, glutamyl, or GlcNAc residue. A minor carbonyl group signal from label observed at 195 ppm (*27*) is attributed to catabolism of the β-methylene carbon of dopamine to an aldehyde group, perhaps 3,4-dihydroxybenzaldehyde (*1*).

Solid-state NMR analysis of *M. sexta* pupal cuticle provides direct evidence that aromatic cross-links derived from catecholamines stabilize the chitin-protein matrix during the process of sclerotization. Covalent bonds form between carbons of the catechol ring and nitrogens of the imidazole ring of cuticular proteins. That chitin may also be involved in the cross-link structure is indicated by tight binding of the histidyl-catecholamine adduct to chitin isolated from cuticle by hot alkali extraction. Solid-state NMR data on natural-abundance ^{13}C in protein, chitin, catechol, and lipid during cuticulogenesis support the general scheme (*1, 2*) for assembly of the pupal procuticle with increasing amounts of protein and chitin secreted after ecdysis as well as the gradual accumulation of catechols during sclerotization.

REFERENCES AND NOTES

1. H. R. Hepburn, in *Comprehensive Insect Physiology, Biochemistry and Pharmacology*, G. A. Kerkut and L. I. Gilbert, Eds. (Pergamon, New York, 1985), vol. 3, p. 1; S. O. Andersen, *ibid.*, p. 59; K. J. Kramer, C. Dziadik-Turner, D. Koga, *ibid.*, p. 75; G. J. Blomquist and J. W. Dillwith, *ibid.*, p. 117; N. F. Hadley, *Sci. Am.* **254**, 104 (July 1986).
2. P. C. J. Brunet, *Insect Biochem.* **10**, 467 (1980); H. Lipke, M. Sugumaran, W. Henzel, *Adv. Insect Physiol.* **17**, 1 (1984).
3. G. S. Jacob, J. Schaefer, G. E. Wilson, Jr., *J. Biol. Chem.* **258**, 10824 (1983); *ibid.* **260**, 2777 (1985).
4. J. Schaefer and E. O. Stejskal, *J. Am. Chem. Soc.* **98**, 1031 (1976).
5. *Manduca sexta* were reared as described by R. A. Bell and F. G. Joachim [*Ann. Entomol. Soc. Am.* **69**, 365 (1976)] and by J. P. Reinecke, J. S. Buckner, and S. R. Grugel [*Biol. Bull.* **158**, 129 (1980)].
6. Cuticular samples (200 to 300 mg) were prepared at 4°C by bisecting pupae or adults sagittally and quickly removing all internal tissues with forceps. Cuticles or exuviae were rinsed briefly in cold distilled water, lyophilized, and ground into a powder (40 to 60 mesh, Wiley micromill).
7. Assignment of resonances was made by comparison to solution and solid-state spectra of model compounds and cuticle [A. Allerhand, *Acc. Chem. Res.* **11**, 469 (1978); G. C. Levy, R. L. Lichter, G. L. Nelson, *Carbon-13 Nuclear Magnetic Resonance Spectroscopy* (Wiley, New York, ed. 2, 1980); M. G. Peter, L. Grun, H. Forster, *Angew. Chem. Int. Ed. Engl.* **24**, 638 (1984); K. J. Kramer *et al.*, *UCLA (Univ. Calif. Los Angeles) Symp. Mol. Cell. Biol.*, in press.
8. G. S. Jacob, J. Schaefer, E. O. Stejskal, R. A. McKay, *J. Biol. Chem.* **260**, 5899 (1985).
9. H. R. Hepburn and D. C. Roberts, *J. Insect Physiol.* **21**, 1741 (1974); S. O. Andersen, *Annu. Rev. Biochem.* **24**, 29 (1979); M. L. Kiely and L. M. Riddiford, *Roux's Arch. Rev. Biol.* **194**, 325 (1985); J. Doctor, D. Fristrom, J. W. Fristrom, *J. Cell Biol.* **101**, 189 (1985).
10. On the basis of relative concentrations of cuticular components from Fig. 1 and from gravimetric analysis, newly ecdysed *M. sexta* pupal cuticle is approximately 14% protein, 2% chitin, 1% catechol, 3% lipid, and 80% water. Sclerotized cuticle (3 days after ecdysis) is 20% protein, 25% chitin, 3.5% catechol, 1.5% lipid, and 50% water. Pupal exuvium is 32% protein, 36% chitin, 18% catechol, 5% lipid, and 9% water. NMR spectra were normalized for direct intensity comparison of lyophilized samples.
11. Labeled histidine (10 to 14 mg) (99% atomically labeled ^{15}N, MSD Isotopes, Montreal, Canada) was dissolved in 0.3 ml of water, the *p*H was adjusted to 6.8, and the solution was filtered through a 0.5-μm Millex-PF filter (Millipore, Bedford, Massachusetts), and injected into a wandering fifth-instar larva through an abdominal proleg.
12. M. Alla and E. Lippmaa, *Chem. Phys. Lett.* **37**, 260 (1976); S. J. Opella and M. H. Frey, *J. Am. Chem. Soc.* **101**, 5854 (1979).
13. See, for example, G. C. Levy and R. L. Lichter, *Nitrogen-15 Nuclear Magnetic Resonance Spectroscopy* (Wiley, New York, 1979); M. Witanowski, L. Stefaniak, G. A. Webb, in *Annual Reports in NMR Spectroscopy*, G. A. Webb, Ed. (Academic Press, New York, 1981), vol. 11B.
14. A. Odier, *Mem. Soc. Hist. Nat. (Paris)* **1**, 29 (1823); T. Fukamizo *et al.*, *Arch. Biochem. Biophys.* **249**, 15 (1986). Chitin was prepared by repeatedly boiling finely ground cuticle (5 mg ml^{-1}) 10 or 20 times for 1 hour each in 1*M* sodium hydroxide and washing with water.
15. M. Munowitz *et al.*, *J. Am. Chem. Soc.* **104**, 1192 (1982).
16. Sclerotized pupal cuticle has more chitin than protein (*9*). The maximum histidine content of *M. sexta* cuticular protein is about 10% (K. J. Kramer, unpublished observation), of which one-third is recoverable in the chitin preparation. Therefore, less than 3% of the chitin preparation can be histidine, and less than 1%, the aromatic-imidazole carbons of histidine.
17. J. Schaefer, R. A. McKay, E. O. Stejskal, *J. Magn. Reson.* **34**, 443 (1979); J. Schaefer, E. O. Stejskal, J. R. Garbow, R. A. McKay, *ibid.* **59**, 150 (1984).
18. DCPMAS NMR spectra were obtained by using matched spin-lock transfers first from ^1H to ^{13}C, and then from ^{13}C to ^{15}N. If the ^{15}N radio-frequency field is on resonance and its amplitude satisfies a magic-angle-spinning carbon-nitrogen Hartmann-Hahn condition (*17*), a spin-lock transfer from ^{13}C to ^{15}N drains polarization from ^{13}C. A direct difference experiment between single and double cross-polarization procedures therefore results in the accumulation of DCPMAS difference ^{13}C signals arising exclusively from ^{13}C directly bonded to ^{15}N. The fraction of ^{13}C with ^{15}N neighbors can be determined quantitatively from such difference spectra.
19. To label cuticular chitin with ^{13}C, 400 mg of [^{13}C(U)] D-glucose (90% atomically labeled, MSD Isotopes, Montreal, Canada) were admixed with 2 g of artificial diet and fed to each larva.
20. The carbon-nitrogen contact was maintained for 3 msec, during which time the polarization transfer from a carbonyl carbon to an amide nitrogen is only half completed.
21. The ^{15}N distribution for this sample was intermediate to those shown in Fig. 2, B and C; the total ^{15}N incorporation was greater than for the pupal exuviae sample, although less per milligram of tissue.
22. To label catechols, 5 mg of [*ring*-$^{13}C_6$]dopamine (99% atomically labeled, MSD Isotopes, Montreal Canada) dissolved in 0.05 ml of water were injected into a wandering-stage larva.
23. J. B. Stothers, *Carbon-13 NMR Spectroscopy* (Academic Press, New York, 1972).
24. T. L. Hopkins, T. D. Morgan, Y. Aso, K. J. Kramer,

Science **217**, 364 (1982); T. L. Hopkins, T. D. Morgan, K. J. Kramer, *Insect Biochem.* **14**, 533 (1984); T. D. Morgan *et al.*, *ibid.*, in press; C. R. Roseland, J. M. Green, L. M. Riddiford, *J. Insect Physiol.* **32**, 473 (1986).
25. M. D. Sefcik, E. O. Stejskal, R. A. McKay, J. Schaefer, *Macromolecules* **12**, 423 (1979).
26. T. Kato, S. Ito, K. Fujita, *Biochim. Biophys. Acta* **881**, 415 (1986).
27. This is an isotropic chemical shift. A minor peak near 190 ppm also appears in the spectrum of the *ring*-^{13}C labeled cuticle (Fig. 4F), but this peak is a spinning sideband not removed by pulse techniques because of extensive ^{13}C–^{13}C dipolar coupling among aromatic carbons.
28. Research conducted by U.S. Grain Marketing Research Laboratory, Agricultural Research Service, U.S. Department of Agriculture, in cooperation with Monsanto Company and the Departments of Biochemistry and Entomology, Kansas Agricultural Experiment Station, Manhattan 66506 (contribution 87-51-J). Supported in part by grants 85-CRCR-1-1667 from the USDA Competitive Research Grant Program and PCM-8411408 from the National Science Foundation. Mention of a proprietary product in this paper does not imply approval by the USDA to the exclusion of other products that may also be suitable.

2 September 1986; accepted 15 December 1986

Isolation and Structure of a Covalent Cross-Link Adduct Between Mitomycin C and DNA

MARIA TOMASZ,* ROSELYN LIPMAN, DONDAPATI CHOWDARY, JAN PAWLAK, GREGORY L. VERDINE,† KOJI NAKANISHI*

A DNA cross-link adduct of the antitumor agent mitomycin C (MC) to DNA has been isolated and characterized; the results provide direct proof for bifunctional alkylation of DNA by MC. Exposure of MC to *Micrococcus luteus* DNA under reductive conditions and subsequent nuclease digestion yielded adducts formed between MC and deoxyguanosine residues. In addition to the two known monoadducts, a bisadduct was obtained. Reductive MC activation with $Na_2S_2O_4$ (sodium dithionite) leads to exclusive bifunctional alkylation. The structure of the bisadduct was determined by spectroscopic methods that included proton magnetic resonance, differential Fourier transform infrared spectroscopy, and circular dichroism. Formation of the same bisadduct in vivo was demonstrated upon injection of rats with MC. Computer-generated models of the bisadduct that was incorporated into the center of the duplex B-DNA decamer d(CGTACGTACG)$_2$ indicated that the bisadduct fit snugly into the minor groove with minimal distortion of DNA structure. A mechanistic analysis of the factors that govern monofunctional and bifunctional adduct formation is presented.

THE POTENT ANTITUMOR AGENT MITOMYCIN C (MC, **1**) is one of the few antibiotics known to react covalently with DNA in vivo and in vitro (*1*). Thus exposure of DNA to MC results in irreversible association of the MC chromophore with that of the DNA (*2*) and in altered

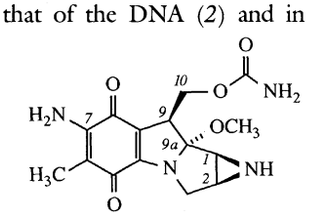

MC, **1**

renaturation kinetics due to putative formation of interstrand cross-links (*3*). However, since the proposed bifunctional cross-link or cross-links account for only a small fraction of the MC bound to DNA (*4, 5*), monofunctional binding is the major pathway under conditions that have normally been used.

The DNA-alkylating function of MC can be activated by two mechanisms: (i) reductive activation by bacterial and mammalian reductases or chemical reducing agents (*6–8*), and (ii) acidic activation by mild aqueous acid (*9, 10*). The structure of the major monofunctional adduct isolated from an MC-DNA complex has only recently been characterized as N^2-(2″β,7″-diaminomitosen-1″α-yl)-2′-deoxyguanosine (**2a**) (*11, 12*), a compound previously isolated from a model reaction and fully elucidated by spectroscopy (*13–16*). Adduct **2a** accounted for more than 90% of the MC bound to calf thymus DNA when the reductive activating agents NADPH–cytochrome c reductase/NADPH, xanthine oxidase/NADH, or H_2/PtO_2 were used in vitro; two minor N^2-dG adducts, **2b** and **3**, were also characterized. However, in that none of the above compounds corresponded to a mitosene adduct (M)(*12*) bearing two attached nucleoside units ("cross-link"), the bifunctional adduct or adducts may have been formed in amounts too low for HPLC-UV detection. We found that the reducing system influences how MC reacts, whether as a monofunctional or bifunctional DNA-alkylating agent. We secured sufficient amounts of a bisadduct from reactions of MC with *Micrococcus luteus* DNA to fully characterize this bifunctional MC-DNA adduct.

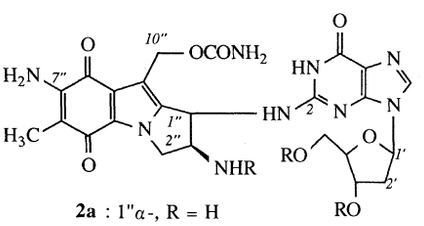

2a : 1″α-, R = H

2b : 1″ß-, R = H

2c : 1″α-, R = Ac

2d : 1″ß-, R = Ac

3 : 1″α-, R = H, 10″ substituent = -OH

Figure 1 shows HPLC traces of digestion mixtures that arose from MC–*M. luteus* DNA and MC-poly(dG-dC) complexes (*17*) that were formed under reductive activation by H_2/PtO_2 or $Na_2S_2O_4$. Activation of MC by H_2/PtO_2 (Fig. 1A) resulted in the production of four adducts from *M. luteus*

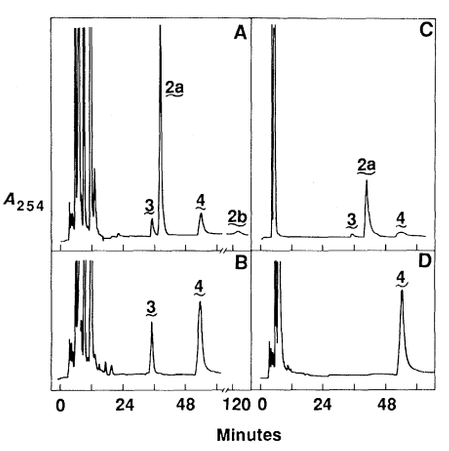

Fig. 1. HPLC patterns from DNase I, SVD, and alkaline phosphatase digest of various MC-DNA and MC-poly(dG-dC) complexes. (**A** and **B**) Digests of MC–*M. luteus* DNA complexes formed under reductive activation by H_2/PtO_2 and $Na_2S_2O_4$, respectively. (**C** and **D**) Digests of MC-poly(dG-dC) formed under reductive activation by H_2/PtO_2 and $Na_2S_2O_4$, respectively. Column: Beckmann Ultrasphere ODS, 1.0 by 25 cm; flow rate: 2.0 ml/min; eluant: 8/92 (v/v) CH_3CN/0.02*M* potassium phosphate, *p*H 5.0; detection: UV band at 254 nm (A_{254}).

M. Tomasz, R. Lipman, D. Chowdary, Department of Chemistry, Hunter College, City University of New York, New York, NY 10021.
J. Pawlak, G. L. Verdine, K. Nakanishi, Department of Chemistry, Columbia University, New York, NY 10027.

*Correspondence may be addressed to either of these authors.

†Present address: Department of Chemistry, Massachusetts Institute of Technology, Cambridge, MA 02139.